Combustion of Metallic Iron in Solid Propellants

James C. Thomas, Gavin D. Lukasik, Felix A. Rodriguez,
Waruna D. Kulatilaka and Eric L. Petersen
J. Mike Walker '66 Department of Mechanical Engineering, Texas A&M University
College Station, TX, USA 77843

1 Introduction

Composite solid propellants are generally composed of ammonium perchlorate (AP) and a fuel/binder (e.g., hydroxyl-terminated polybutadiene – HTPB) and are widely utilized in the propulsion industry. Metal fuels can be added to the propellant to increase their heat of combustion, density, combustion temperature, and specific impulse [1]. However, condensed combustion products (CCPs) resulting from metal combustion can adversely affect vehicle performance through two-phase losses in the nozzle or deposition within the combustion chamber [1].

Aluminum is the most widely studied metal fuel additive in solid propellant systems owing to its high performance, easy availability, low toxicity, and good stability [2]. In general, aluminum particles accumulate on the surface of burning propellants where they can sinter, coalesce, and agglomerate into larger particles. Aluminum agglomeration characteristics largely depend on propellant formulation variables, especially AP concentration and size distribution, but also on operating conditions (e.g., pressure, burning rate, etc.). 'Pocket' models, which estimate the space available between coarse AP particles, have historically been utilized to predict Al agglomerations characteristics with relatively good accuracy since Al tends to agglomerate on the fuel surface between large oxidizer particles. [3-4] Quantitative experimental techniques to characterize aluminum agglomeration characteristics have historically only included quench bomb studies, wherein agglomerates ejected from the propellant surface are captured in a quenching liquid or disk and analyzed *ex-situ* with microscopy techniques. However, modern optical techniques [5-9] have allowed for direct visualization of agglomeration processes *in-situ* and determination of particle size and velocity distributions, but these efforts have been limited to ambient or very low pressures.

In comparison to Al, iron (Fe) has the potential to provide better performance (specific impulse and density specific impulse), as illustrated with the chemical equilibrium analysis (CEA) computations presented in Fig. 1. In addition, although the authors can find no record of previous mention in the literature, Fe can serve as a chlorine scavenging agent (forms $FeCl_3$ gas), virtually eliminating the presence of toxic hydrochloric acid (HCl) in the exhaust products of AP-based propellants. However, the inclusion of Fe in composite propellants has not been sufficiently explored in the open literature. This observation is potentially due to iron's poor aging stability and rapid formation of oxides at normal storage conditions, but modern preparation methods allow for the production of stable Fe additives with hydrocarbon surface coatings [10] which mitigate these issues. Thus far, evaluation of iron for composite

Correspondence to: James.Chris.Thomas@tamu.edu

propellants has been limited to a few decomposition experiments [11-13] and two limited strand burner studies [13-14]. The potential of Fe as an additive in solid propellants is clear but has not been sufficiently evaluated thus far. In the current study, the fundamental combustion behavior of Fe micro-particles in composite AP/HTPB/AP laminate propellant samples burning at elevated pressure is investigated with high-speed, high-magnification video methods coupled with automated particle tracking analysis techniques. Provided first is an overview of the experimental methods, namely the propellant and sample formulation and the optical diagnostics and image post-processing. The results are then presented, including burning rates, qualitative flame behavior, and particle analyses.

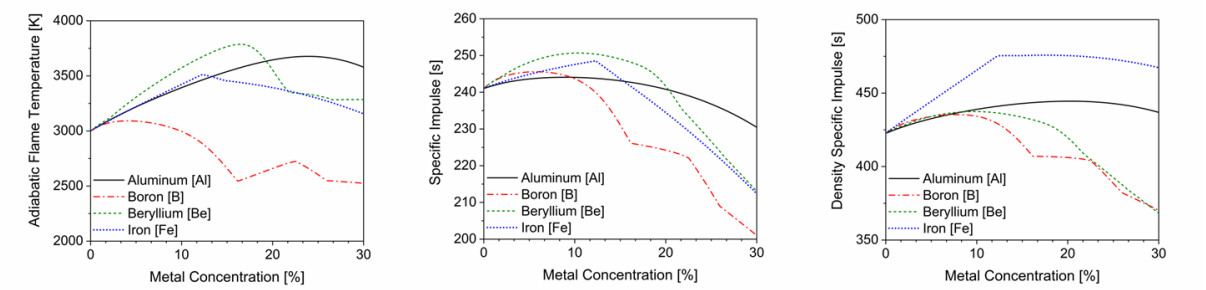

Figure 1: Theoretical performance of selected metal fuels (Al, B, Be, and Fe) in composite AP/HTPB propellant systems with 90% solids concentration.

2 Experimental Methods

2.1 Propellant Formulation

A series of CEA computations were completed to optimize the Fe loading for highest performance (c^* and I_{sp}). CEA computations were completed at a pressure of 6.89 MPa, assuming shifting equilibrium chemistry, a vacuum exit condition, and perfect nozzle expansion. The heat of formation of propellant-grade, IPDI-cured HTPB ($C_{213.8}H_{323.0}O_{4.6}N_{2.3}$ – 342 kJ/mol) was taken from Thomas and Petersen [15]. The optimized propellant formulation consists of 13% binder, 75% AP, and 12% Fe by mass. This Fe-loaded propellant formulation has a theoretical adiabatic flame temperature, characteristic velocity, specific impulse, and density specific impulse of 3364 K, 1537 m/s, 250 s, and 462 s, respectively. The corresponding fuel mixture (excluding AP) consists of 52% binder and 48% Fe. This fuel mixture is utilized as the fuel lamina composition here to emulate the full propellant formulation in ballistic testing.

2.2 Sample Preparation

Laminate propellant sample preparation procedures have been previously provided by the authors [16-17] and are briefly described here for completeness. Circular AP pellets (1.27 cm × 1.6 mm) were pressed at 55 kN for one hour. Tape spacers (2 or 4 mil) were utilized to set the fuel lamina spacing. A pre-mixed and vacuumed fuel slurry was added between two AP pellets, covered in cellophane wrap, and cured at elevated temperature (65 °C, 1 day). A small fraction of cure catalyst (DBTDL) was included in the fuel. The cured sample was sanded to its final dimensions: 12.7 × 6.35 × ~3.175 cm. Fuel lamina thickness (135 ± 15 μm) was confirmed with an optical microscope.

2.3 Ballistic Testing

Laminate propellant samples were burned in a constant-volume strand burner in an inert atmosphere (N_2) at elevated pressure (~6.89 MPa). Detailed ballistic testing procedures have been previously provided by the authors [16-17]. Samples were ignited with a stoichiometric B:KNO_3 mixture and Nichrome wire. Steady-state combustion processes were monitored with a high-magnification (3.83 μ/pixel, 512×1024 resolution) system consisting of a high-speed camera (Photron FASTCAM SA3 120K) coupled with a long-distance microscope (K2 DistaMax, CF-2 objective). Natural flame luminosity was the only light required for clear imaging, and no external light source was implemented.

2.4 Data Reduction Techniques

The authors have previously provided qualitative analysis of particle agglomeration behavior and measured burning rates by manually tracking the leading-edge flames (LEFs) in aluminized laminate propellant samples [16-17]. In the current study, an in-house image processing algorithm was established based on a recent suspended particle tracking code [18] to characterize burning rates as well as the size and velocity of particles and agglomerates. The processing algorithm consists of three main steps: segmentation, identification, and tracking. In the segmentation step, unprocessed frames from the high-speed video were transformed into a binary format based on a constant light intensity threshold, which isolates ejected particles and removes the propellant sample and background from further analysis. Neighboring pixels corresponding to particles were subsequently grouped together in the identification step. Very small (< 100 pixels) and large (> 9000 pixels) groups were removed to avoid analysis of noise and capturing of the propellant flame, respectively. Particle size (i.e., diameter) was computed based on a spherical particle approximation and the video resolution (i.e., microns/pixel). The flame front was tracked by relaxing the large pixel grouping restriction and considering the lowest tracked pixel as the regressing propellant surface. A representative set of images illustrating the image processing technique is shown in Fig. 2, where the left image is unprocessed, the middle image illustrates segmentation, and the right image depicts tracking of the flame front and tracked particles. The dashed red line corresponds to the vertical position of the flame front, and the solid yellow lines correspond to individual particle trajectories.

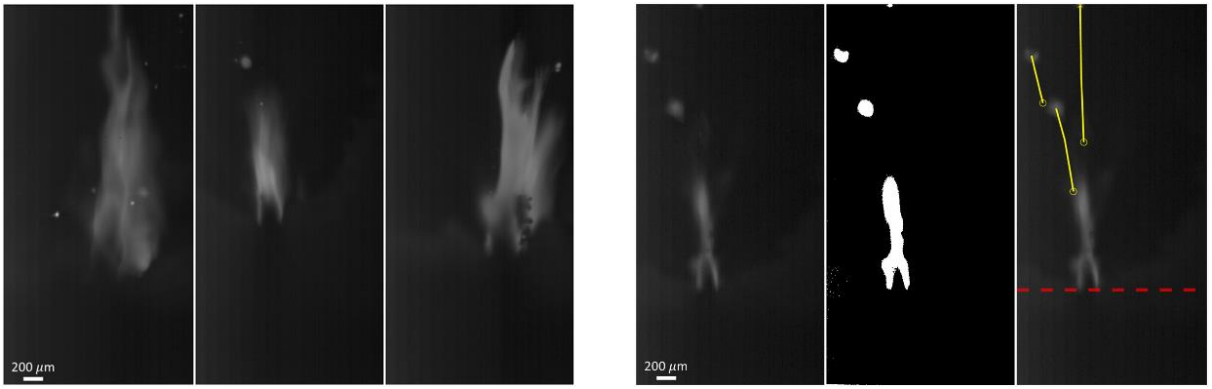

Figure 2: (left) Representative still frames from the combustion of laminate propellant samples containing Fe microparticles. (right) Representative high-speed video still frames depicting the image processing steps: (1) unprocessed, (2) segmented, and (3) identified/tracked.

3 Results and Discussion

3.1 Burning Rate Measurements

Burning rates for laminate propellant samples with fuel lamina composed of plain HTPB and HTPB loaded with 48% Fe microparticles are provided in Fig. 3. The data shown in the left plot of Fig. 3 were manually tracked from high-speed videos. The propellant's flame front location is plotted against time, and the slope of the transient data represents the burning rate of the sample. The measured burning rates for the plain HTPB and Fe-loaded samples were 3.90 ± 0.15 mm/s and 5.02 ± 0.28 mm/s, respectively. Small differences in the observed burning rate for similar propellant formulations can be attributed to minor variations in the fuel lamina thickness (± 15 μm) and testing pressure (± 0.05 MPa). The addition of Fe microparticles to the fuel lamina significantly increases ($\sim$30%) the sample burning rate.

Flame front location data tracked manually and by the image processing algorithm are compared in the right plot of Fig. 3 for Fe-loaded propellant samples. Excellent agreement was observed between the two techniques, indicating the surface tracking algorithm performed well. Deviations from the expected

behavior were occasionally observed when large particles were ejected from the regressing propellant surface causing local distortions or alterations to the local light emission.

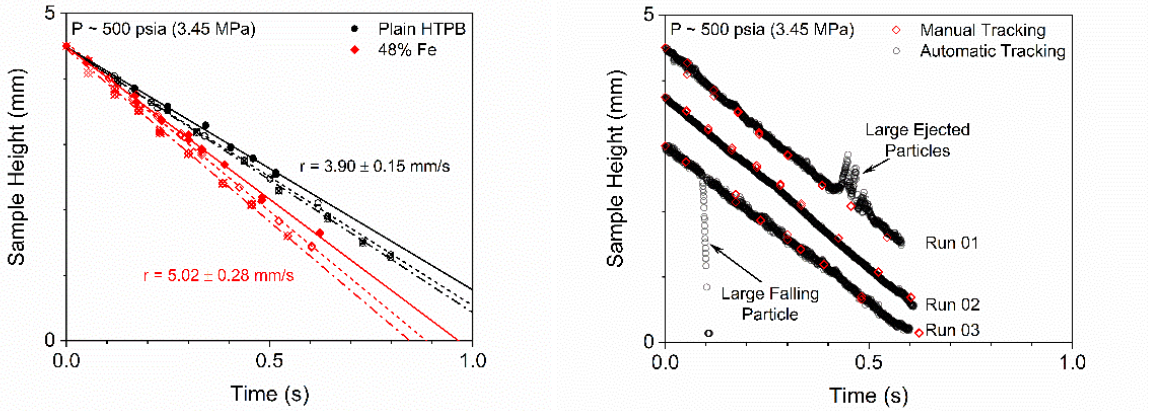

Figure 3: (left) Manually and (right) automatically tracked burning rates for laminate propellant samples with a fuel lamina (t~135 μm) composed of plain HTPB or HTPB loaded with 48% Fe particles.

3.2 Qualitative Combustion Behavior

Select still frames from the combustion of laminate propellant samples containing Fe microparticles are shown in Fig. 2. At the experimental conditions evaluated herein (t~135 μm, P~3.45 MPa), the fuel lamina extends above the oxidizer/fuel interface on the order of 250-500 μm. Additive particles generally aggregate, sinter, and agglomerate on the fuel lamina surface prior to ejection at the fuel lamina's tip, yielding ejected particles that are larger than the initial additive particle size (~45 μm). However, the additive particles may also eject at the oxidizer/fuel interface or from the fuel lamina without aggregating or agglomerating. The observed aggregation and agglomeration behavior are analogous to those observed in the literature for aluminum particles. Furthermore, agglomeration processes taking place solely on the fuel lamina suggest the standard 'pocket' agglomeration models developed for aluminum-loaded propellants [3-4] may be applicable to similar formulations containing iron. In general, the additive particles ejected from the surface glow brighter than their surroundings, indicating they may be reacting at a higher temperature, even near the propellant surface.

Analysis of the high-speed video (see Fig. 2) indicates that a significant portion of the fuel lamina is covered by CCPs during steady-state combustion. Korotkith et al. [13] observed that CCPs ejected from an AP/HTPB solid propellant containing nano-Al and nano-Fe were composed of a small portion of unreacted Al (< 2%), Fe_3C (< 5%), C_3N_4, and Al_2O_3. Based on Korotkith et al.'s [13] observations and a series of temperature-dependent CEA computations of HTPB/Fe mixtures, the present authors expect the surface CCPs to be composed mostly of molten iron and iron carbide (Fe_3C).

The significant increase in burning rate (~30%) accompanying the addition of a high concentration (48%) of Fe microparticles to the fuel mixture is somewhat surprising. Although Korotkith et al. [13] and Styborski et al. [14] noted increases in burning rates with nano-Fe additives, their studies included the additive at lower concentrations. The presence of a surface CCP layer is expected to block heat transfer to the virgin propellant. However, this deficiency appears to be overcome, potentially by an increased flame temperature and near-surface additive reactions, as indicated by 'glowing' particles leaving the regressing propellant surface.

3.3 Particle Size, Velocity, and Acceleration Measurements

Particle size distributions measured for particles/agglomerates ejected from the surface of a burning laminate propellant sample containing Fe microparticles are shown in the left plot of Fig. 4. Many of the particles are near the initial additive particle size, indicated by a dashed black line. The presence of particles smaller than this value suggests the additive may react near the propellant surface, which agrees

with previous observations made herein. Larger particles are expected from the aggregation and agglomeration processes. Most of the larger particles are smaller than 135 μm, which is the thickness of the flame lamina, indicating its size limits most agglomeration processes. However, a few larger agglomerations (200-500 μm) are also observed. Good repeatability for the measured particle size distribution is observed between the experiments. Several potential sources of error in the estimation of accurate particle/agglomerate sizes exist. The authors believe the particle size distributions presented herein are highly accurate, with an estimated relative error for individual measurements on the order of $\pm$5%.

Particle velocity distributions are shown in the middle plot of Fig. 4. Particles/agglomerates are accelerated away from the regressing propellant surface by local gas movement after they are ejected from the surface. Accordingly, their acceleration is controlled and their maximum velocity is bounded by the local combustion gas velocities, which can be theoretically estimated by the application of mass conservation with corresponding estimates for local gas and decomposition conditions at the fuel lamina surface (see dashed lines in the middle plot of Fig. 4). As expected, the observed particle velocities fall well below the estimated maximum gas velocity, since particle acceleration and terminal velocity are dictated by a balance of drag and gravitational forces acting on the particle. In general, larger particles were ejected at lower velocities, which is expected considering their larger inertia. In addition, particle acceleration, and presumably the corresponding drag force acting on the particle, can be estimated by considering the transient velocity of a single particle, as shown in the right plot of Fig. 4.

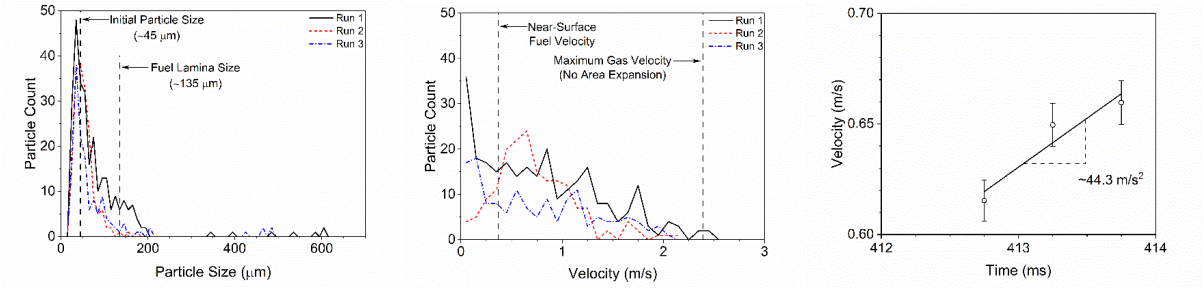

Figure 4: (left) Size distribution of particles and agglomerates ejected from the surface of laminate propellant sample from three separate experiments. (middle) Distribution of velocities for particles and agglomerates ejected from the surface of laminate propellant samples from three separate experiments. (right) Estimation of velocity and acceleration for a single particle.

4 Conclusion

Iron represents a potential high-performance additive for solid propellant systems that has not been investigated in detail. The current study included combustion testing of laminate propellant samples loaded with Fe microparticles in an optically accessible bomb. Combustion behavior was probed with a high-speed, high-magnification imaging system, and an in-house image processing algorithm was developed to measure burning rates and ejected particle/agglomerate sizes and velocities. The addition of Fe to the fuel lamina yielded a substantial increase in the global burning rate (~30%), even at the high concentration evaluated herein. High-speed video analysis indicated additive particles ejecting at the oxidizer/fuel interface or agglomerating on the fuel lamina surface prior to ejection. The fuel lamina thickness appears to control the formation and size of the largest agglomerates. Particle velocities are controlled by a balance of gravitational forces, drag forces imparted by expanding combustion product gases, and inertia of the particle. The experimental methods presented herein represent significant improvements to standard techniques since they provide time-resolved, statistically significant particle size and velocity distribution data with a simple 2D system. In addition, these methods allow for characterization at elevated pressure, which has proved difficult in previous experimental efforts. Future work will focus on refinement of the experimental techniques developed herein and characterization of alternative metal-loaded propellant formulations at elevated pressure

References

[1] Sutton GP, Biblarz O. (2017) Rocket Propulsion Elements, John Wiley and Sons (ISBN 9781118753651)

[2] DeLuca LT (2018) Overview of Al-Based Nanoenergetic Ingredients for Solid Rocket Propulsion. Def. Technol. 14: 357.

[3] Maggi F, DeLuca LT, Bandera A (2015) Pocket Model for Aluminum Agglomeration Based on Propellant Microstructure. AIAA J. 53: 3395.

[4] Gallier S (2009) A Stochastic Pocket Model for Aluminum Agglomeration in Solid Propellants. Propell. Explos., Pyrotech. 34: 97.

[5] Guildenbecher DR, Cooper MA, Gill W, Stauffacher HL, Oliver MS, Grasser TW (2014) Quantitative, Three-Dimensional Imaging of Aluminum Drop Combustion in Solid Propellant Plumes via Digital In-Line Holography. Opt. Lett. 39: 5126.

[6] Chen Y, Guildenbecher DR, Hoffmeister KNG, Cooper MA, Stauffacher HL, Oliver MS, Washburn EB (2017) Study of Aluminum Particle Combustion in Solid Propellant Plumes Using Digital In-Line Holography and Imaging Pyrometry. Combust. Flame. 182: 225.

[7] O'Neil AM, Demko A, Petersen EL, Kulatilaka WD (2019) Ultrashort-Pulse LIBS for Detecting Airborne Metals During Energetic Reactions. Appl. Opt. 58: 79.

[8] O'Neil MO, Niemiec NA, Demko A, Petersen EL, Kulatilaka WD (2018) Laser-Induced-Breakdown-Spectroscopy-Based Detection of Metal Particles Released into the Air During Combustion of Solid Propellants. Appl. Opt. 57: 1910.

[9] Marsh AW, Wang GT, Heyborne JD, Guildenbecher DR, Mazumdar YC (2021) Time-Resolved Size, Velocity, and Temperature Statistics of Aluminum Combustion in Solid Rocket Propellants. Proc. Combust. Inst. 38: 4417.

[10] Bunker CE, Karnes JJ (2004) Low-Temperature Stability and High-Temperature Reactivity of Iron-Based Core-Shell Nanoparticles. J. Am. Chem. Soc. 126: 10852.

[11] Gromov A, Strokova Y, Kabardin A, Vorozhtsov A, Teipel U (2009) Experimental Study of the Effect of Metal Nanopowders on the Decomposition of HMX, AP, and AN. Propell. Explos., Pyrotech. 34: 506.

[12] Nair S, Mathew S, Nair RCP (2020) Impact of Lattice Inclusion of Cu and Fe Ions on Thermal Decomposition Characteristics of Ammonium Perchlorate. PeerJ Inorg. Chem. 2: 1.

[13] Korotkikh AG, Glotov OG, Sorokin IV, Arkhipov VA (2020) Chap. 7: Bimetal Fuels for Energetic Materials. Innovative Energetic Materials: Properties, Combustion Performance and Application. Springer (ISBN 9789811548307).

[14] Styborski JA, Scorza MJ, Smith MN, Oehlschlaeger MA (2015) Iron Nanoparticle Additives as Burning Rate Enhancers in AP/HTPB Composite Propellants. Propell. Explos., Pyrotech. 40: 253.

[15] Thomas JC, Petersen EL (2021) HTPB Heat of Formation: Literature Survey, Group Additive Estimation, and Theoretical Effects. AIAA J. 60: 1269.

[16] Thomas JC, Rodriguez FA, Sammet T, Dillier CA, Petersen ED, Petersen EL (2019) Manufacturing and Burning of Composite AP/HTPB/AP Laminate Propellants. AIAA Paper 2019-4365.

[17] Thomas JC, Rodriguez FA, Petersen EL (2020) Strand Burner Experiments with Metal Loaded AP/HTPB Laminate Propellants. AIAA Paper 2020-1429.

[18] Lukasik G, Rogers J, Kota KR, Wilkerson JW, Lacy TE, Kulatilaka WD (2021) Application of Digital Particle Tracking and Schlieren Imaging to Study Debris Cloud and Shockwave Formation During Hypervelocity Impacts. AIAA Paper 2021-0725.